PROPERTIES AND RARE PRODUCTION AND DECAY PROCESSES OF THE HIGGS BOSON IN CMS*

Michał Bluj

on behalf of the CMS Collaboration

National Centre for Nuclear Research, Poland

Received 13 April 2025, accepted 16 April 2025, published online 26 June 2025

This report summarises measurements of the Higgs boson properties performed with the CMS experiment at the CERN LHC. The measurements presented here base on data from *pp* collisions at the center-of-mass energy of 7, 8, and 13 TeV collected up to the year 2018 and corresponding to integrated luminosity of 5, 20, and 138 fb^{-1}, respectively. These results represent the most up-to-date knowledge on the Higgs boson properties. All presented measurements agree with predictions of the Standard Model of particle physics within their uncertainties.

DOI:10.5506/APhysPolBSupp.18.5-A6

1. Introduction

Since the discovery of the Higgs boson (H) in 2012 [1–3], its properties have been tested with increasing precision. In this report, we summarize the most up-to-date knowledge on the Higgs boson properties based on measurements performed using *pp* collision data collected with the CMS detector [4] at the LHC in two periods: 2010–2012 (Run 1) and 2015–2018 (Run 2). During Run 1, LHC operated at the center-of-mass energy of 7 and 8 TeV and the CMS experiment collected, respectively, 5 and 20 fb^{-1} of data, while during Run 2, the center-of-mass energy amounted to 13 TeV and integrated luminosity of CMS data to 138 fb^{-1}.

2. Higgs boson mass

The mass of the Higgs boson, m_H, is a free parameter of the Standard Model of particle physics (SM) and, within the SM, its value determines all the other Higgs boson properties.

* Presented at the 31st Cracow Epiphany Conference on the *Recent LHC Results*, Kraków, Poland, 13–17 January, 2025.

Precise measurements of m_H are performed using two fully-reconstructed, high-resolution ($\mathcal{O}(1\%)$) decay channels: $H \to \gamma\gamma$ and $H \to ZZ \to 4\ell$ (reconstructed mass shown in Fig. 1). The most recent combination of m_H measurements using these two channels performed by the CMS Collaboration with Run 1 and 2016 Run 2 data amounts to $m_H = 125.38 \pm 0.14\,[\pm 0.11(\mathrm{stat.}) \pm 0.09(\mathrm{syst.})]$ GeV [5, 6]. The uncertainty of the measurement is dominated by its statistical component, similarly to the earlier measurements using only Run 1 data. It was achieved thanks to precise calibration of photon energy and lepton momentum. This combined measurement was recently improved by a measurement with the $H \to ZZ \to 4\ell$ channel using the full Run 2 data set which yields $m_H = 125.08 \pm 0.12\,[\pm 0.10(\mathrm{stat.}) \pm 0.05(\mathrm{syst.})]$ GeV [7]. The precision of m_H determination can be further improved combining measurements with both channels with more data.

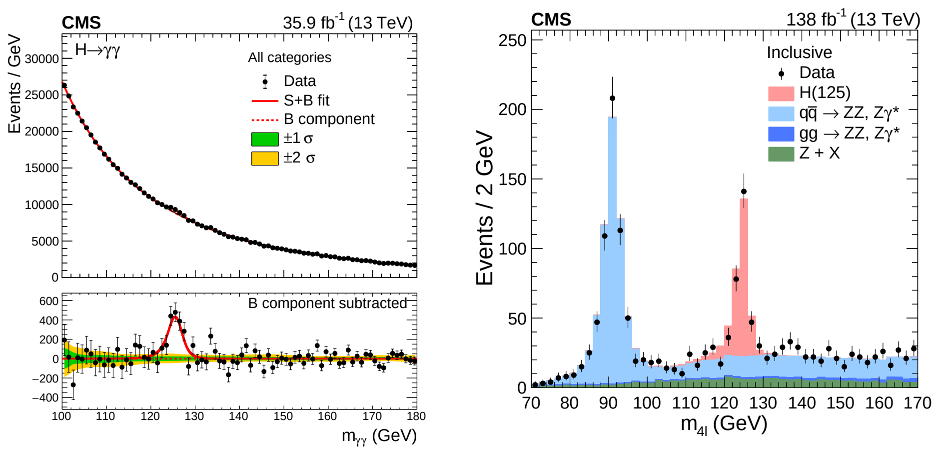

Fig. 1. Distributions of mass of photon pairs, $m_{\gamma\gamma}$ (left) [6] and of four leptons, $m_{4\ell}$ (right) [7].

3. Total width of the Higgs boson

Another important parameter describing the Higgs boson is its total width, Γ_H. In the SM, its value amounts to 4.1 MeV for the observed value of m_H [8]. Deviation from the SM expectation will be a sign of non-SM decays of the H boson. The predicted value of Γ_H is much smaller than the experimental resolution and direct measurements from the line shape with the $H \to \gamma\gamma$ and $H \to ZZ \to 4\ell$ decays give only weak upper limits of around 1 GeV (see *e.g.* Ref. [5]). Therefore, an indirect method was proposed in Refs. [9, 10] where Γ_H is obtained by comparing the on- and off-shell production of the $H \to VV$ ($V = W, Z$) process as given in Eq. (1)

$$\sigma^{\text{on-shell}}_{gg\to H\to VV} \propto \frac{g^2_{ggH}g^2_{HVV}}{m_H\Gamma_H}\,,$$
$$\sigma^{\text{off-shell}}_{gg\to H^*\to VV} \propto \frac{g^2_{ggH}g^2_{HVV}}{(2m_V)^2}\,. \tag{1}$$

This method assumes that the couplings of the Higgs boson are the same for both on- and off-shell productions. It was firstly employed by the CMS Collaboration to measure Γ_H using a combination of $H \to ZZ \to 4\ell$ and $H \to ZZ \to 2\ell 2\nu$ processes with a partial Run 2 data set [11]. The most recent measurement of Γ_H performed by the CMS Collaboration exploits the two final states with the full Run 2 data set [7] and gives $\Gamma_H = 3.0^{+2.0}_{-1.5}$ MeV (Fig. 2) and $\Gamma_H < 330$ MeV at the 95% confidence level (C.L.). The measured value agrees with both the previous measurement and the SM prediction, and constitutes the most precise measurements of Γ_H to date. The uncertainties of the measurement are dominated by the statistical component (on off-shell yields) that will decrease with including more data. The measurements will also profit from reducing the uncertainty of the theoretical prediction on the non-resonant production of ZZ pairs which is the main irreducible background for the off-shell $H^* \to ZZ$ signal.

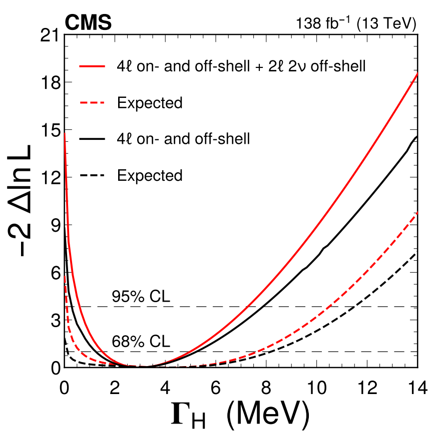

Fig. 2. Profile likelihood scan of the H boson width (Γ_H) measured using the on- and off-shell $H \to ZZ$ production [7].

4. Production and decays

The Higgs boson analyses at the LHC measure directly only signal yields for a given combination of production and decay modes. However, the production and decay rates, and then individual couplings can be determined with a combination of all the analyses exploiting different correlations between production and decay modes to which the different channels are sensitive, considering the theory and experimental correlations among them. Such a combination requires a set of basic theory assumptions which are discussed in Ref. [12].

The CMS Collaboration performed combined measurements exploiting all analyses based on 13 TeV data collected in 2016–2018 [13]. Production (μ_i) and decay (μ^f) signal strength parameters (a ratio of the measured production or decay rate to the SM predictions) extracted with the combined analysis are shown in Fig. 3, all in agreement with the SM expectations. Signal strengths for the main production and decay modes are measured with a precision up to about 10%: for the gluon–gluon fusion, it is better than 10%, while for other production processes, it amounts to 10–20%. The signal strength for the main bosonic decay modes ($H \to \gamma\gamma, ZZ, WW$) and for $H \to \tau\tau$ is measured with an uncertainty of about 10%, and about 20% for $H \to b\bar{b}$ decays. Decay rates of rare $H \to \mu\mu$ and $H \to Z\gamma$ processes are known with much higher uncertainties given the very low branching ratio of these decay modes.

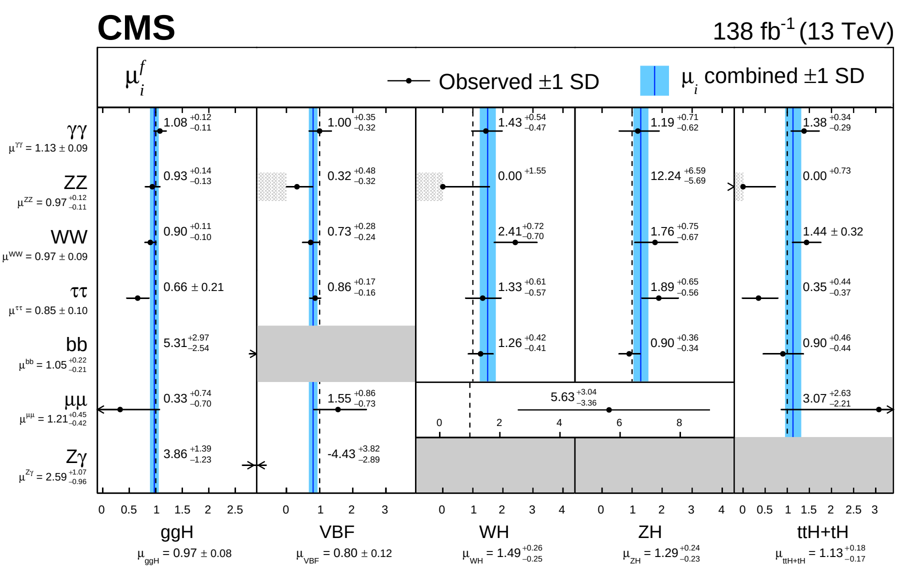

Fig. 3. Signal strength parameters measured for various production modes (μ_i) and decay channels (μ^f) [13].

4.1. Rare $H \to \mu\mu$ and $H \to Z\gamma$ decays

The $H \to \mu\mu$ decay, with $\mathcal{B}(H \to \mu\mu) = 2.18 \times 10^{-4}$, provides the experimentally most sensitive probe at the LHC to the Yukawa coupling to the second-generation fermions. The most recent CMS search for this process exploits the mass of muons pairs ($m_{\mu\mu}$) in categories targeting the main production modes, using the whole Run 2 data set [14]. Observed distribution of $m_{\mu\mu}$ (for all event categories combined) is shown in Fig. 4, left. An excess of events over the background expectation was observed with a significance of 3.0 standard deviations (s.d.), where the expectation for the SM Higgs boson was 2.5 s.d. The corresponding signal strength amounts to $\mu = 1.19^{+0.40}_{-0.39}(\text{stat.})^{+0.15}_{-0.14}(\text{syst.})$ and is shown in Fig. 4, right for individual event categories compared with the expectation for the SM Higgs boson. This result is the first evidence of the decay of the Higgs boson to the second-generation fermions.

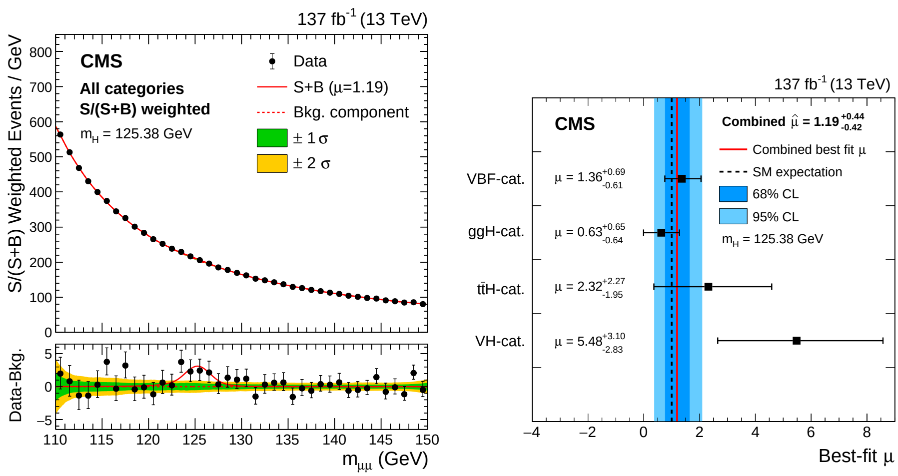

Fig. 4. Left: the $m_{\mu\mu}$ distribution for the combination of all event categories. Right: the signal strength in each $H \to \mu\mu$ event category (black points) and their combination (solid red line) compared with the SM expectation (dashed grey line) [14].

The $H \to Z\gamma$ decay is a loop-mediated process with a relatively small branching fraction of $\mathcal{B} = 1.5 \times 10^{-3}$ predicted by the SM which can be enhanced in the case of exchanging new particles postulated in several beyond-SM scenarios. In the search for the $H \to Z\gamma$, the Z boson is reconstructed through $Z \to \ell\ell$ ($\ell = e, \mu$) decays, and then the signal is identified as a narrow peak in the distribution of the mass of the $\ell\ell\gamma$ system ($m_{Z\gamma}$). To enhance the sensitivity, events are divided into categories with different signal-to-background ratios utilising the kinematic properties of different H-production modes. The most recent result is a combination of searches preformed by the ATLAS and CMS collaborations with data collected during Run 2 [15]. Figure 5, left shows the observed distribution of $m_{Z\gamma}$ for all event categories in the ATLAS and CMS analyses combined. This combination constitutes the first evidence for the $H \to Z\gamma$ decay with an observed significance of 3.4 s.d. (Fig. 5, right). The observed signal strength equals $\mu = 2.2 \pm 0.6(\text{stat.}) \pm 0.3(\text{syst.})$ which leads to the branching fraction of $\mathcal{B}(H \to Z\gamma) = (3.4 \pm 1.1) \times 10^{-3}$. This result agrees with the SM prediction within 1.9 s.d.

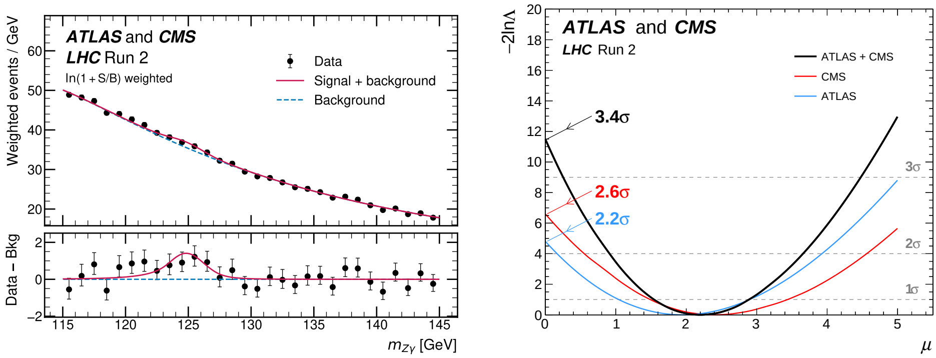

Fig. 5. The $m_{Z\gamma}$ distribution for the weighted combination of all event categories in the ATLAS and CMS analyses (left) and the profile likelihood as a function of the signal strength of the $H \to Z\gamma$ decay (right) [15].

5. Couplings

The measurements can also be parametrised in terms of coupling modifiers, κ, that scale the SM couplings of H to other particles [12]. The quantities such as production cross sections (σ_i) and decay widths (Γ^f) are scaled by κ^2. In the case of loop-mediated processes, *e.g.* $gg \to H$ or $H \to \gamma\gamma$, two approaches are considered: they are either treated as effective and parametrised with their own κ modifiers or they are resolved assuming SM-like contributions. By construction, in the SM, all κ values are equal to one. Results of the combined coupling measurement are summarised in Fig. 6 and are in all cases consistent with the expectations for the SM Higgs boson.

5.1. Coupling to charm quark

After establishing evidence of the $H \to \mu\mu$ decay, which allowed to obtain the Higgs-to-muon coupling, the interest focuses on coupling to the charm quark. Several ways to probe this coupling are explored.

The $H \to c\bar{c}$ decay constitutes the "golden" channel. However, despite its branching fraction of $\mathcal{B}(H \to c\bar{c}) = 2.8\%$ it is much higher than for decay to muons, a search for the $H \to c\bar{c}$ decay is extremely challenging

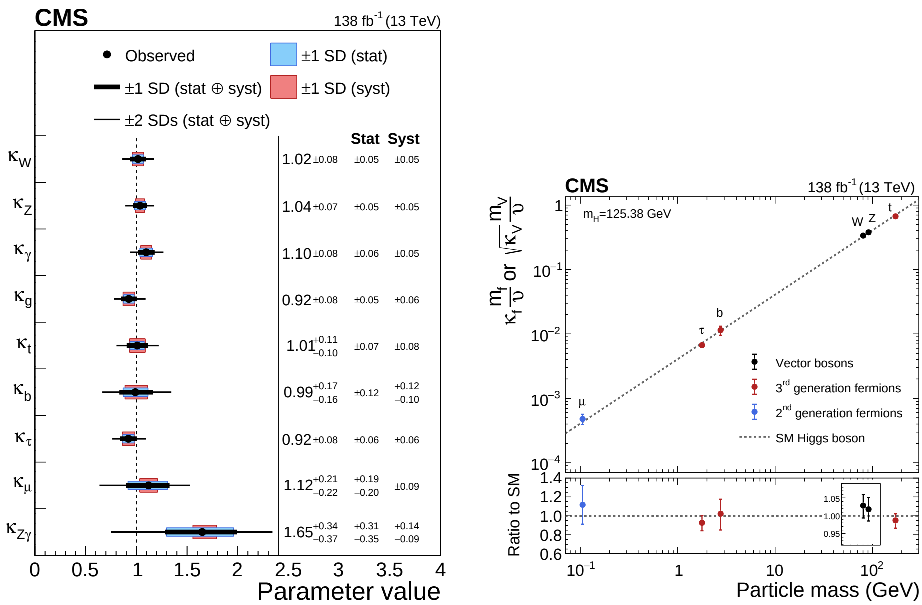

Fig. 6. Individual coupling modifiers (left) and reduced couplings as a function of a particle mass (right) [13].

due to an overwhelming background from copious production of quark and gluon jets at the LHC, and the difficulty of identifying c-quark jets, including distinguishing them from b-quark jets. To cope with those challenges, a strategy similar to those in the well-established $H \to b\bar{b}$ studies was employed: the associated VH ($V = W, Z$) production is used with a highly-boosted V-boson decaying leptonically (combining events with 0, 1 or 2 charged leptons), two topologies with "resolved" and "merged" c-jets are combined, and the $VZ(\to c\bar{c})$ is exploited as a standard candle. In addition, the most recent CMS analysis [16] with the entire Run 2 data uses current state-of-the-art machine learning algorithms to identify c-jets in both topologies and to reconstruct the mass of the $c\bar{c}$ pair (Fig. 7, left). The analysis allowed for the first observation of the $VZ(Z \to c\bar{c})$ process at a hadron collider with a significance of 5.7 s.d. with a signal strength of $\mu_{VZ(Z\to c\bar{c})} = 1.01^{+0.2}_{-0.21}$, which ensures validity of methods used. The observed upper limit on $\sigma(VH)\mathcal{B}(H \to c\bar{c})$ is 0.94 pb at the 95% C.L., corresponding to 14 times the SM prediction (Fig. 7, right). This is interpreted as an observed interval for the Higgs-charm coupling modifier (κ_c) of $1.1 < |\kappa_c| < 5.5$ at the 95% C.L., the most stringent to date.

Another approach is to search for very rare $H \to \psi(nS)\gamma$ ($\psi(nS) = J/\psi, \psi(2S)$) decays mediated by c-quark loops and characterised by a branching fraction of $\mathcal{O}(10^{-6})$, followed by the decay of the $\psi(nS)$ meson to a pair

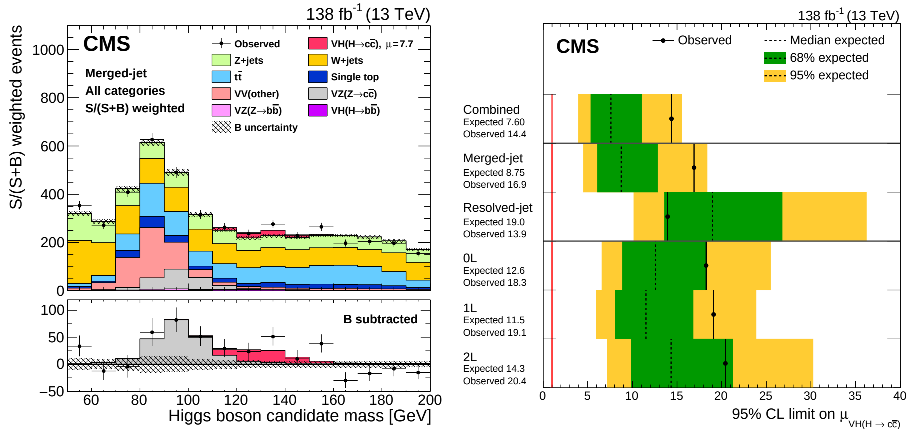

Fig. 7. The combined $m_{c\bar{c}}$ distribution for all "merged-jet" event categories (left), and exclusion limits on the signal strength $\mu_{VH(H\to c\bar{c})}$ at the 95% C.L. (right) [16].

of muons [17]. The signal forms a narrow peak in the mass distribution of the di-muon and photon system ($m_{\mu\mu\gamma}$), as depicted in Fig. 8, left. The sensitivity is then enhanced by categorising events into categories targeting different production processes. A similar approach is used to hunt for Higgs boson to light-quark couplings with $H \to \rho/\phi/K^* + \gamma$ decays which have even smaller branching fractions [18]. Thanks to the low background, the excellent muon momentum and photon energy resolutions of the CMS detector, this channel provides a better signal-to-background ratio than the

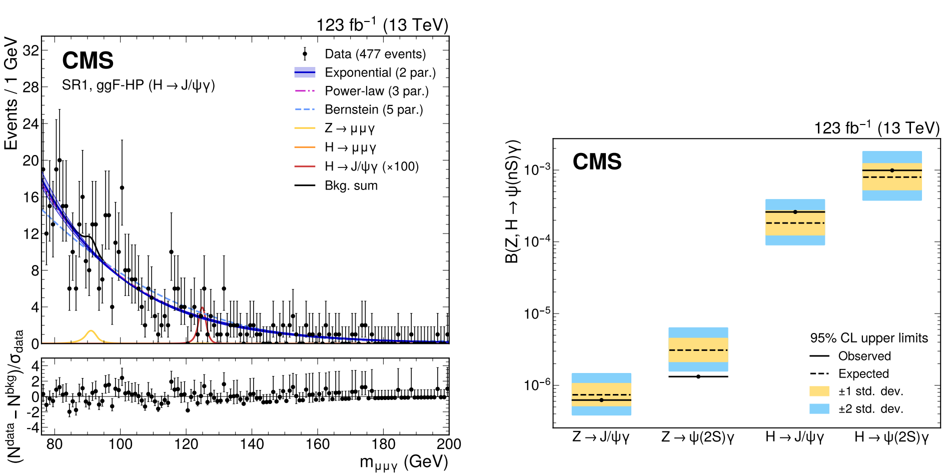

Fig. 8. The $m_{\mu\mu\gamma}$ distribution for one of the event categories (left) and exclusion limits on the branching fractions of the $Z/H \to \psi(nS)\gamma$ (right) [17].

$H \to c\bar{c}$ decay. The main factors limiting the sensitivity are the low event yields and the resonant processes with H that decay through quark loops without the intermediate resonant $c\bar{c}$ state. Current exclusion limits on $\mathcal{B}(H \to \psi(nS)\gamma)$ are of $\mathcal{O}(10^{-4})$ as shown in Fig. 8, right, and translate on the allowed interval of $-166 < \kappa_c < 208$ at the 98% C.L.

Another promising method to access the charm Yukawa coupling is a measurement of the associated cH production. The CMS Collaboration attempted such a measurement with the $H \to \gamma\gamma$ decays using Run 2 data [19]. The cross section predicted by the SM amounts to only $\sigma_{cH} = 90$ fb. The main background sources are the continuous di-photon production, $\gamma +$jets process, and the resonant background due to other Higgs boson production mechanisms. Selected events were categorised with two multivariate discriminators, one against continuous and another resonant background, and then a peak in di-photon mass ($m_{\gamma\gamma}$) was searched for (Fig. 9). The data were compatible with the background-only hypothesis and an upper limit at the 95% C.L. on the cH signal strength was set at 243 times the SM prediction. This is then translated to a constraint on c-quark coupling of $|\kappa_c| < 38.1$. The sensitivity of this analysis is dominated by the limited amount of data, theoretical uncertainties of modelling the cH production, and heavy-flavour-related uncertainties of the $gg \to H$ production.

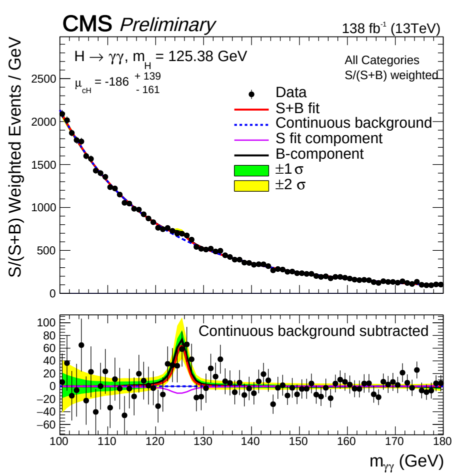

Fig. 9. The $m_{\gamma\gamma}$ distribution for the selected cH events in all categories combined [19].

Yet different approach is to probe the Higgs-charm coupling by exploiting kinematics of the Higgs boson production as proposed in Ref. [20]. The CMS Collaboration performed such an analysis using combined measurements of the differential production cross sections with $H \to \gamma\gamma$, $H \to ZZ \to 4\ell$,

$H \to WW \to 2\ell 2\nu$, and $H \to \tau\tau$ decay channels [21]. Distribution of the production cross section as a function of the Higgs boson transverse momentum ($p_{\rm T}^{H}$) is shown in Fig. 10, left. The observed distribution agrees with the SM predictions within uncertainties. Figure 10, right presents constraints on coupling modifiers of the b- and c-quark (κ_b and κ_c) assuming their dependence of branching fractions. Those translate on the limit on c-quark coupling of $|\kappa_c| < 4$. Similar constraints without the dependence of branching fractions are weaker and lead to an allowed range of $-7 < \kappa_c < 9$.

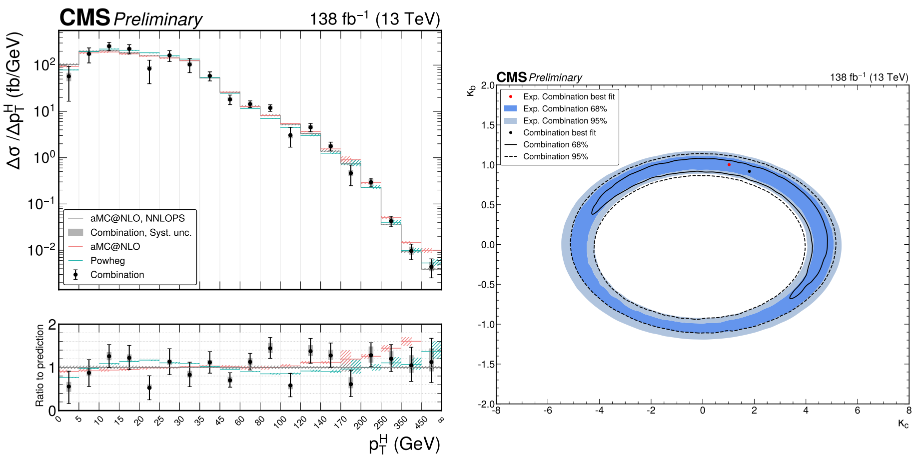

Fig. 10. The total differential cross section as a function of $p_{\rm T}^{H}$ (left), and constraints on coupling modifiers of b- and c-quark (κ_b and κ_c) assuming a coupling dependence of the branching fractions (right) [21].

5.2. *The H boson self-coupling*

The Higgs boson self-coupling (λ) defines the shape of the Higgs potential. In the SM, its value is determined by m_H and the Fermi constant. The value of λ can be probed directly through the Higgs boson pair production (HH). This process, however, is not yet established experimentally due to its low cross section which is three orders of magnitude smaller than that of the single-H production. The results of the search for the HH process are therefore expressed as an upper limit on its cross section that amounts to 3.5 times the SM prediction at the 95% C.L. (Fig. 11, left) [22]. This result can be translated to an allowed range of the Higgs boson self-coupling modifier (κ_λ) of $-1.39 < \kappa_\lambda < 7.02$ at the 95% C.L. (Fig. 11, right).

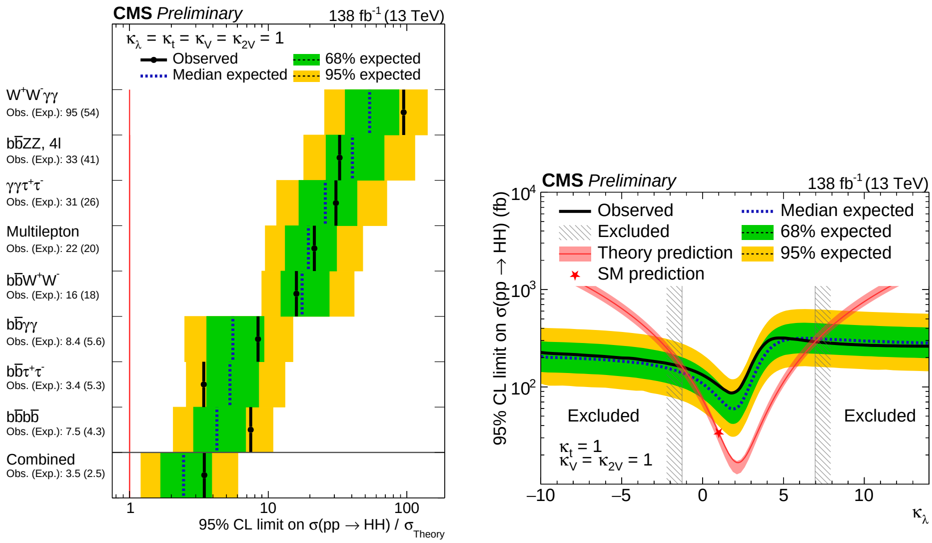

Fig. 11. Exclusion limits on the Higgs boson pair production cross section in searches using different final states and their combination (left), and the 95% C.L. upper limit on the cross section as a function of κ_λ (right) [22].

6. Summary

In this report, we summarised measurements of the Higgs-boson properties performed using data collected with the CMS detector up to 2018. The obtained results represent the most up-to-date knowledge on the Higgs-boson properties. The mass of the Higgs boson (a free parameter of the SM) is measured with a precision of about 0.1%. The observed value of the total width of H (extracted using the on- and off-shell $H \to ZZ$ process) is measured with an uncertainty of about 50% and agrees with the SM prediction. Measured production and decay rates as well as extracted couplings to other particles also agree with predictions of the SM within their uncertainties. The CMS Collaboration looks forward to analysing the full data set of the ongoing Run 3 of the LHC that is expected to more than double amount of collected data, and to the high-luminosity LHC with the upgraded CMS detector, improved theory calculations and analysis techniques which will enable precise measurements with rare processes.

We would like to thank the organizers for the invitation and for making the 31$^{\text{st}}$ Cracow Epiphany Conference a true success. This contribution is partly supported by the Ministry of Science and Higher Education, Poland, grant No. 2022/WK/14.

REFERENCES

[1] ATLAS Collaboration (G. Aad *et al.*), *Phys. Lett. B* **716**, 1 (2012).

[2] CMS Collaboration (S. Chatrchyan *et al.*), *Phys. Lett. B* **716**, 30 (2012).

[3] CMS Collaboration (S. Chatrchyan *et al.*), *J. High Energy Phys.* **2013**, 081 (2013).

[4] CMS Collaboration (S. Chatrchyan *et al.*), *J. Instrum.* **3**, S08004 (2008).

[5] CMS Collaboration (A. Sirunyan *et al.*), *J. High Energy Phys.* **2017**, 047 (2017).

[6] CMS Collaboration (A. Sirunyan *et al.*), *Phys. Lett. B* **805**, 135425 (2020).

[7] CMS Collaboration (A. Hayrapetyan *et al.*), `arXiv:2409.13663 [hep-ex]`, accepted by *Phys. Rev. D*.

[8] LHC Higgs Cross Section Working Group (D. de Florian *et al.*), `arXiv:1610.07922 [hep-ph]`.

[9] F. Caola, K. Melnikov, *Phys. Rev. D* **88**, 054024 (2013).

[10] J.M. Campbell, R.K. Ellis, C. Williams, *Phys. Rev. D* **89**, 053011 (2014).

[11] CMS Collaboration (A. Tumasyan *et al.*), *Nature Phys.* **18**, 1329 (2022).

[12] LHC Higgs Cross Section Working Group (J.R. Andersen *et al.*), `arXiv:1307.1347 [hep-ph]`.

[13] CMS Collaboration (A. Tumasyan *et al.*), *Nature* **607**, 60 (2022).

[14] CMS Collaboration (A. Sirunyan *et al.*), *J. High Energy Phys.* **2021**, 148 (2021).

[15] ATLAS, CMS collaborations (G. Aad *et al.*), *Phys. Rev. Lett.* **132**, 021803 (2024).

[16] CMS Collaboration (A. Tumasyan *et al.*), *Phys. Rev. Lett.* **131**, 061801 (2023).

[17] CMS Collaboration (A. Hayrapetyan *et al.*), *Phys. Lett. B* **865**, 139462 (2025), `arXiv:2411.15000 [hep-ex]`.

[18] CMS Collaboration (A. Hayrapetyan *et al.*), *Phys. Lett. B* **862**, 139296 (2025).

[19] CMS Collaboration, «CMS Physics Analysis Summary», CMS-PAS-HIG-23-010, `https://cds.cern.ch/record/2905239`

[20] F. Bishara, U. Haisch, P.F. Monni, E. Re, *Phys. Rev. Lett.* **118**, 121801 (2017).

[21] CMS Collaboration, «CMS Physics Analysis Summary», CMS-PAS-HIG-23-013, `https://cds.cern.ch/record/2905139`

[22] CMS Collaboration, «CMS Physics Analysis Summary», CMS-PAS-HIG-20-011, `https://cds.cern.ch/record/2917252`